



TITLE:

# Non-destructive method for wood identification using conventional X-ray computed tomography data

AUTHOR(S):

Kobayashi, Kayoko; Hwang, Sung-Wook; Okochi, Takayuki; Lee, Won-Hee; Sugiyama, Junji

---

CITATION:

Kobayashi, Kayoko ...[et al]. Non-destructive method for wood identification using conventional X-ray computed tomography data. Journal of Cultural Heritage 2019, 38: 88-93

ISSUE DATE:

2019-7

URL:

<http://hdl.handle.net/2433/241782>

RIGHT:

© 2019 Les Auteurs. Publi e par Elsevier Masson SAS. Cet article est publi e en Open Access sous licenceCC BY (<http://creativecommons.org/licenses/by/4.0/>).



Available online at  
**ScienceDirect**  
[www.sciencedirect.com](http://www.sciencedirect.com)

Elsevier Masson France  
**EM|consulte**  
[www.em-consulte.com](http://www.em-consulte.com)



## Original article

# Non-destructive method for wood identification using conventional X-ray computed tomography data



Kayoko Kobayashi<sup>a,\*</sup>, Sung-Wook Hwang<sup>a</sup>, Takayuki Okochi<sup>b</sup>, Won-Hee Lee<sup>c</sup>,  
Junji Sugiyama<sup>a,d,\*</sup>

<sup>a</sup> Research Institute for Sustainable Humanosphere, Kyoto University, Uji, Kyoto 611-0011, Japan

<sup>b</sup> National Institute for Cultural Properties Nara, Nara 630-8577, Japan

<sup>c</sup> Department of Wood and Paper Science, College of Agriculture and Life Sciences, Kyungpook National University, Daegu 41566, South Korea

<sup>d</sup> College of Materials Science and Engineering, Nanjing Forestry University, Nanjing 210037, Jiangsu, PR China

## INFO ARTICLE

### Historique de l'article :

Reçu le 18 septembre 2018

Accepté le 4 février 2019

Disponible sur Internet le 23 February 2019

### Keywords :

Gray-level co-occurrence matrix

Local binary pattern

Image database

X-ray computed tomography

Tripitaka Koreana

## ABSTRACT

We establish an efficient and reliable method of wood identification that combines a non-destructive and non-invasive laboratory-scale tool, X-ray computed tomography (CT), with machine learning for image recognition. We selected six hardwood species used to create the Tripitaka Koreana and obtained the X-ray CT data of its woodblocks. Image recognition systems using the gray-level co-occurrence matrix (GLCM) or local binary patterns (LBP) were applied to the CT images and the prediction accuracies were evaluated. Because the gray level of the CT data is linearly related with the density, the CT images were preprocessed to calibrate the density. Although the resolution of the images is too low for the anatomical microstructures required for wood identification to be easily recognized visually, the predicted accuracies are quite high in both systems. However, the LBP system has slight advantages over the GLCM system. The results moreover show that the calibration of gray level to density improves the accuracies of the results. If the candidates for the wood species are selected properly and sufficient data for training is available, this technique will provide novel information about the properties of wooden historical objects.

© 2019 Les Auteurs. Publié par Elsevier Masson SAS. Cet article est publié en Open Access sous licence CC BY (<http://creativecommons.org/licenses/by/4.0/>).

## 1. Introduction

Wood species are generally identified by visual inspection using optical or electron microscopy based on their differences in anatomical features [1,2]. However, this conventional method is destructive and time-consuming because wood samples must be sliced or flattened to expose three different planes: the transverse, radial, and tangential sections. Another difficulty is that identification requires a highly specialized knowledge of wood anatomy. Near infrared (NIR) spectroscopy [3–5], high-resolution X-ray micro computed tomography (CT) [6], and low-resolution X-ray CT combined with image recognition [7] have been proposed as a substitute for situations in which the conventional method is difficult to apply, such as the investigation of registered cultural objects. Low-resolution CT with image recognition is the most versatile and promising of these methods because of the looser res-

trictions on sample size and condition. For instance, the surface of the sample simply needs to be clean and free of paint for NIR spectroscopy, and only tiny samples (less than 1 mm in diameter) are needed for high-resolution CT measurement.

The Tripitaka Koreana is known as the most complete collection of printing blocks of Buddhist texts in Korea. As indicated by its name in Korean, *Palman Daejanggyeong* (Eighty-Thousand Tipitaka), it comprises more than 80,000 wooden printing blocks that were carved in the 13th century to pray for an end to the war with the Mongols. They have been well preserved in a special depository in the temple of Haeinsa, which was designated as a UNESCO World Heritage site in 1995. The wood species used in the woodblocks have been partly investigated by microscopic inspection using small broken fragments [8]. The results show that all the wood species used for the main bodies of the woodblocks are diffuse-porous wood: *Cerasus*, which accounts for more than half of the total, followed by *Pyrus*, *Betula*, *Cornus*, *Acer*, *Machilus*, *Salix*, and *Daphniphyllum*. As the amount of attention paid to the Tripitaka Koreana has increased since it was added to UNESCO's Memory of the World Register in 2007, a complete investigation is expected to comprehensively understand its history and the protection

\* Corresponding authors at: Research Institute for Sustainable Humanosphere, Kyoto University, Gokasho, Uji, Kyoto 611-0011, Japan.

Adresses e-mail : [aka.kobayashi@mail.ecc.u-tokyo.ac.jp](mailto:aka.kobayashi@mail.ecc.u-tokyo.ac.jp) (K. Kobayashi), [sugiyama.junji.6m@kyoto-u.ac.jp](mailto:sugiyama.junji.6m@kyoto-u.ac.jp) (J. Sugiyama).

**Table 1**

List of wood species for gray level calibration.

	Density (g/cm <sup>3</sup> )
<i>Paulownia tomentosa</i>	0.230
<i>Chamaecyparis pisifera</i>	0.291
<i>Populus suaveolens</i>	0.358
<i>Pterocarya rhoifolia</i>	0.369
<i>Picea jezoensis</i>	0.421
<i>Abies firma</i>	0.427
<i>Magnolia obovata</i>	0.485
<i>Trochodendron aralioides</i>	0.514
<i>Betula grossa</i>	0.636
<i>Acer palmatum</i>	0.659
<i>Acer rufinerve</i>	0.660
<i>Quercus acuta</i>	0.909

it requires. To investigate such large quantities of woodblocks, we need to employ a non-destructive and simple analysis method.

We previously evaluated an image recognition system for identifying the wood of the Tripitaka Koreana using the transverse sections of stereograms [9]. The top six wood species comprising the Tripitaka Koreana (*Cerasus*, *Pyrus*, *Betula*, *Cornus*, *Acer*, and *Machilus*) were used for the dataset, and a simple image recognition system with a gray-level co-occurrence matrix (GLCM) [10] and weighted neighbor algorithm [11,12] was applied. Although the images of the diffuse-porous wood species appear similar to each other, wood species were identified correctly with sufficient accuracy when the appropriate preprocessing and parameters were selected. In addition, the result suggests the possibility of application to images with even lower resolutions such as CT images.

## 2. Research aim

Here, we present a practical procedure for non-destructive and non-invasive wood identification, based on the case of the Tripitaka Koreana. The data was obtained using a lab-scale X-ray CT system [13], which was designed for large objects such as the woodblocks. Before investigating the image analysis, the correlation between the image gray levels and densities of the wood samples were investigated because density is an important factor for wood identification. We tested two classic texture analysis methods, GLCM [10] and local binary patterns (LBPs) [14,15], with and without adding density information, and used a k-NN algorithm for classification.

## 3. Experimental

### 3.1. Wood samples

The wood blocks used in the present study are the same as those used in our previous work [9]. Six hardwood species, *Acer pictum*, *Betula costata*, *Cornus controversa*, *Cerasus jamasakura*, *Machilus thunbergi*, and *Pyrus pyrifolia*, were supplied from a collection of the Korea Forestry Promotion Institute or the Xylarium in Kyoto University (KYOW). One specimen was prepared for each species. For gray level calibration, 12 wood blocks with various densities were also selected from KYOW. The densities of the wood blocks were measured gravimetrically (Table 1).

### 3.2. X-ray CT

The CT data was acquired using the micro-focus X-ray CT system, which is an upgraded version of the SMX-100CT-D (Shimadzu Corporation, Japan; [13]). The data was taken with charge-coupled device (CCD) camera at 50 kV and 60  $\mu$ A. To obtain high-resolution data, we used only data from a single line in the CCD camera and constructed the two-dimensional images. The original images were

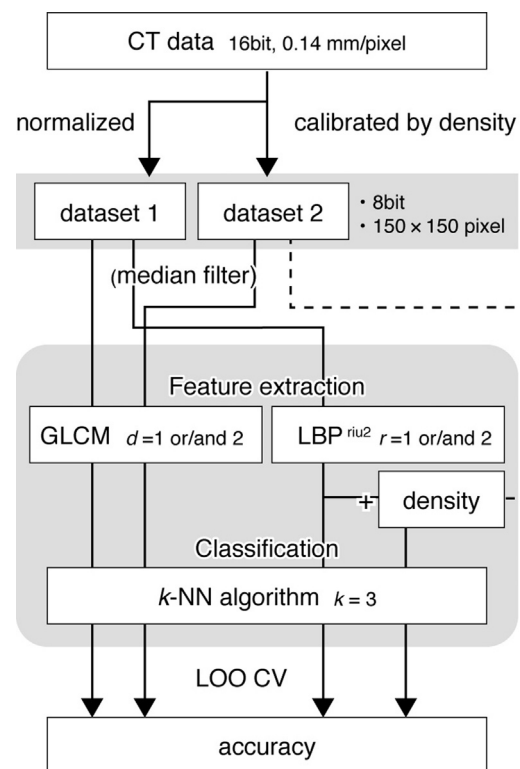


**Fig. 1.** Image recognition procedure.

transverse sections of wood with  $2048 \times 2048$  pixel at 16-bit grayscale, a resolution of  $14.4 \mu\text{m}/\text{pixel}$ , and slice thickness of  $0.35 \text{ mm}$ .

### 3.3. Image recognition procedure

An outline of the image recognition procedure is shown in Fig. 1. All the image and statistical analyses were performed using R version 3.4.2 [16] with the packages “tiff,” [17] “stats,” “class,” [18], and “wvtool” [19]; the latter was developed in our laboratory.

#### 3.3.1. Pretreatments

The  $150 \times 150$  pixel images ( $2.1 \times 2.1 \text{ mm}$  in actual size) were cropped from the original CT data, excluding the center part of the data and the sample edges, where the data was affected by strong artifacts. The transverse section image dataset included 96 to 216 images for each wood species.

The 16-bit gray scale images were subsequently converted to 8-bit grayscale using two methods (datasets 1 and 2). The conversion for dataset 1 was carried out using min-max normalization. The gray levels of dataset 2 were calibrated to the densities by scaling over the range that corresponds to  $0\text{--}1.2 \text{ g}/\text{cm}^3$  using the function, which will be described in section 3.1. A median filter with a radius of 1 pixel was applied to the images in the datasets to remove noise.

#### 3.3.2. Feature extraction and classification

GLCM is a method for calculating the texture features based on the composition of pixel values among the neighboring pixels (Fig. 2a). The composition is described by absolute values; thus, the calculated features depend on how the gray levels were modified during preprocessing. In contrast, LBP features are independent of pixel brightness because they are calculated based on whether a pixel’s gray level is higher or lower than that of its neighboring pixels (Fig. 2b). The LBP patterns are obtained for each pixel by converting the surrounding pixels to binary using the gray level of the center pixel as a threshold. Therefore, GLCMs were calculated

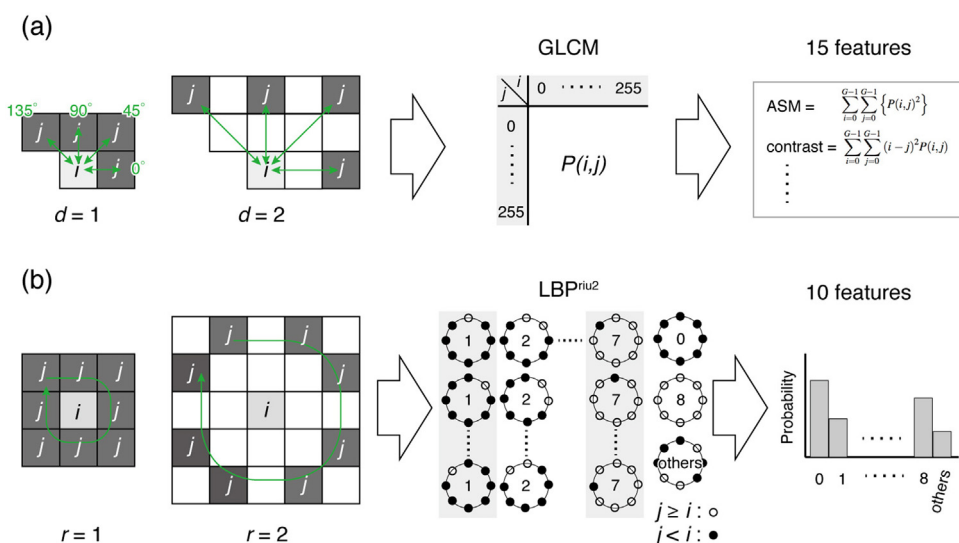


Fig. 2. Feature extraction procedures. (a) GLCM. (b) LBP<sup>riu2</sup>.

from either dataset 1 or dataset 2, whereas LBP features were only calculated from dataset 1 and used the density, which was calculated as the mean of the gray level of the whole image, as an additional feature (Fig. 1).

In the present study, we used rotation-invariant features for both GLCM and LBP. GLCMs were constructed from the average of four directions (0°, 45°, 90°, and 135°) based on the distance between pixels, i.e.,  $d = 1$  or 2. Fifteen texture features (ASM, contrast, IDM, entropy, correlation, variance, sum average, sum entropy, difference entropy, difference variance, sum variance,  $f12$ ,  $f13$ , shade, and prominence) proposed by Haralick et al. [10] and Albregtsen [20] were calculated, as reported previously [7]. For rotation-invariant LBP features, ten LBP<sup>riu2</sup> features were calculated using the radius between pixels  $r = 1$  or 2, as proposed by Ojala et al. [15]. The features were used for classification after standardization.

The  $k$ -nearest-neighbor ( $k$ -NN) with  $k = 3$  was used for the classification algorithm. The  $k$  value was determined empirically. The predicted accuracy was calculated using leave-one-out cross validation.

## 4. Results

### 4.1. Calibration of gray level with respect to density

The average gray level values were measured from the transverse sections, which were  $1 \times 1$  cm in actual size, of the wood blocks listed in Table 1. The correlation between the gray levels and the density was investigated using simple regression (Fig. 3). The result shows the almost perfect linearity with respect to the range of wood densities; the gray level of the CT data can be converted to density using a calibration function.

The original CT data had a 16-bit gray scale, and the data cropped from the wooden part occupied only the small range of the whole data (Fig. 4a). This 16-bit data was converted to 8-bit gray scale using two methods (Fig. 4b). When general normalization was applied, the distribution of the gray level covered the whole range of levels 0–255. In contrast, the histogram of the data calibrated by the function shown in Fig. 3 shifted the distribution to lower gray levels, which made the image darker than the normalized image (Fig. 4b, inset). The typical images of each species thus obtained are shown in Fig. 5. The brightness of the images varies depending on the densities.

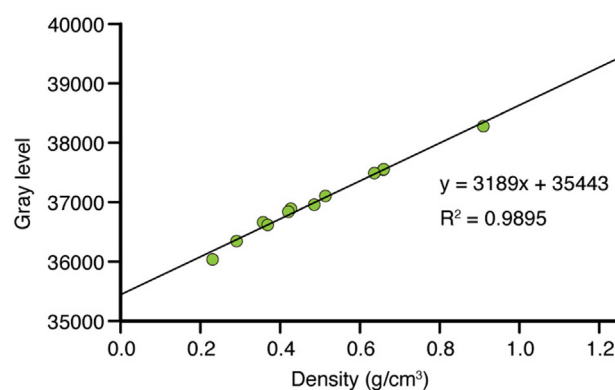


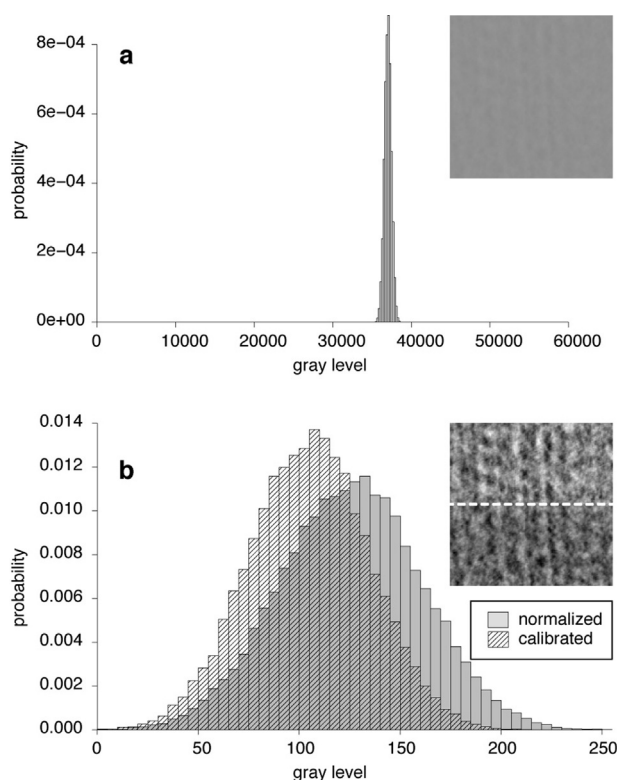
Fig. 3. Correlation between gray level and density. Each point on the plot corresponds to the wood samples listed in Table 1. The line indicates the simple regression with the estimated coefficients and multiple R-squared value.

Compared with the stereograms that we used in the previous study, the information appearing in the CT images is quite different. Because the resolution is approximately 1/20 that of the stereograms, the small vessels are quite unclear in the CT images of *A. pictum*, *C. jamasakura*, and *P. pyrifolia*. In addition, rays, which are one of the most prominent features in the stereograms, are hardly recognizable in the CT images, because there is no significant difference in the density of the rays with respect to other tissues; hence, the images are difficult to rotate such that the rays point in the same direction, as in the previous study [9]. We reported that the anisotropic nature of wood provided helpful information for wood identification, but in the present study, we use the images without this arrangement and calculate rotation-invariant features.

### 4.2. Classification accuracies using GLCM and LBP

The accuracies predicted using the texture features calculated by GLCM are shown in Fig. 6a. While the accuracies are quite high, more than 90%, when either  $d = 1$  or 2 is used, the accuracies increase further when they are both used. The median filter, which was effective for the stereograms in the previous study, does not improve the accuracy here. Dataset 2, which was obtained using the density calibration, yields better results than dataset 1. The wood species with small vessels, i.e., *A. pictum*, *C. jamasakura*, and *P. pyrifolia*, account for most of the misclassifications (Table 2a),

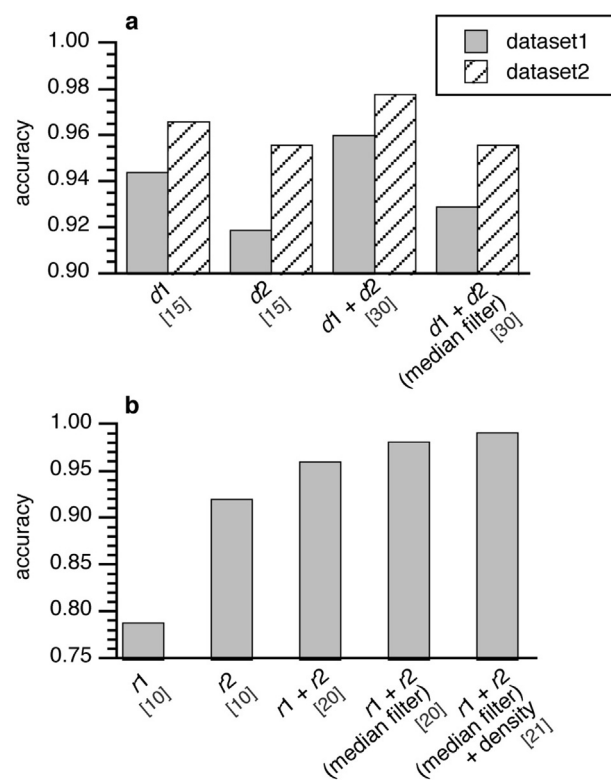




**Fig. 4.** Gray-level histograms of a CT image. Insets show the images corresponding to the histograms. (a) Original 16-bit grayscale image. (b) 8-bit grayscale images after normalization and calibration. The inset in (b) is divided into the normalized image (top) and calibrated image (bottom).

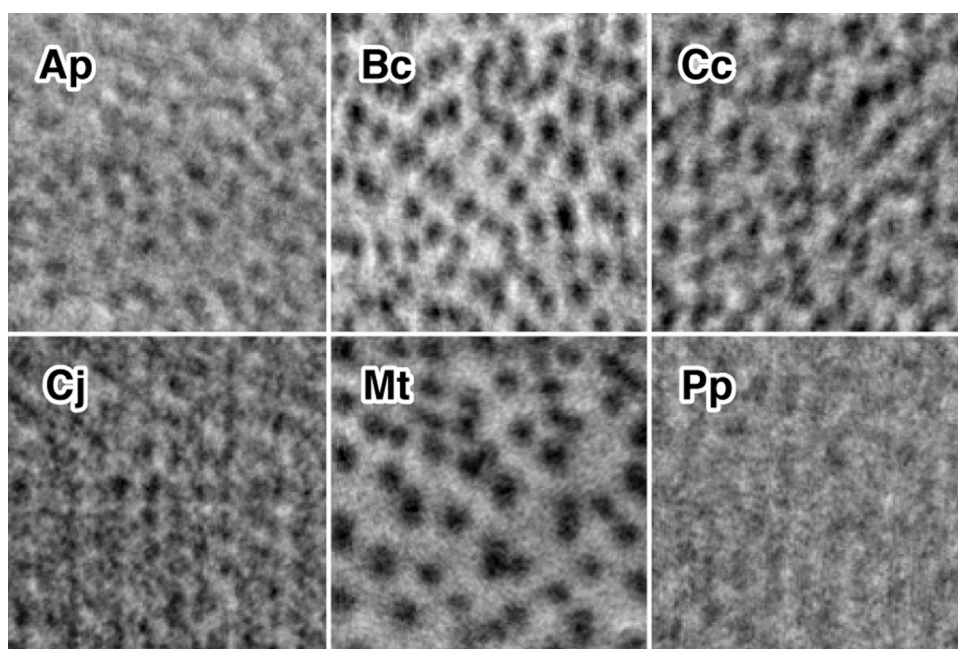
but the density calibration substantially reduces these misclassifications (Table 2b). The density information hence enables the discrimination of wood species with similar textures.

Fig. 6b shows the accuracies predicted when using LBP for the feature extraction. Although the 10 LBP features with  $r=1$  yield low accuracy (less than 80%), the accuracy increases to more than



**Fig. 6.** Predicted accuracies using (a) GLCM and (b) LBP. Numbers in brackets show the number of the texture features.

90% when  $r=2$  is used. Using a combination of these two scales,  $r=1$  and 2, increases the accuracy further. In contrast to the GLCM method, the median filter is effective when used on the LBP features. Adding the density as a feature causes the accuracy to reach 99.5%, which is the highest of the conditions that we tested in this study. Some images of *M. thunbergi* are misclassified as *A. pictum* and *C. controversa* (Table 3); the species misclassified by



**Fig. 5.** Typical images of each species in dataset 2. Ap: *Acer pictum*, Bc: *Betula costata*, Cc: *Cornus controversa*, Cj: *Cerasus jamasakura*, Mt: *Machilus thunbergi*, and Pp: *Pyrus pyrifolia*.

**Table 2**  
Classification table for GLCM with  $d = 1$  and 2.

		True class					
		Ap	Bc	Cc	Cj	Mt	Pp
(a) dataset1							
Predicted class (%)	Ap	95.2	0.0	0.0	0.0	0.0	6.9
	Bc	0.0	97.9	0.5	0.0	0.0	0.0
	Cc	0.0	2.1	99.5	0.0	0.0	0.0
	Cj	1.2	0.0	0.0	94.8	0.0	2.3
	Mt	0.0	0.0	0.0	0.0	100.0	0.0
	Pp	3.6	0.0	0.0	5.2	0.0	90.7
(b) dataset2							
Predicted class (%)	Ap	97.0	0.0	0.0	0.0	0.0	6.0
	Bc	0.0	99.0	0.0	0.0	0.0	0.0
	Cc	0.0	1.0	99.5	0.0	0.0	0.0
	Cj	0.0	0.0	0.5	100.0	0.0	0.0
	Mt	0.0	0.0	0.0	0.0	100.0	0.0
	Pp	3.0	0.0	0.0	0.0	0.0	94.0

**Table 3**  
Classification table for LBP with  $r = 1$  and 2 and the median filter.

		True class					
		Ap	Bc	Cc	Cj	Mt	Pp
(a) without density							
Predicted class (%)	Ap	99.4	0.0	0.9	0.0	4.6	0.0
	Bc	0.0	99.0	0.0	0.0	1.9	0.0
	Cc	0.0	1.0	99.1	0.0	3.7	0.0
	Cj	0.6	0.0	0.0	99.0	0.0	0.0
	Mt	0.0	0.0	0.0	0.0	89.8	0.0
	Pp	0.0	0.0	0.0	1.0	0.0	100.0
(b) with density							
Predicted class (%)	Ap	100.0	0.0	0.0	0.0	1.9	0.0
	Bc	0.0	100.0	0.0	0.0	0.0	0.0
	Cc	0.0	0.0	100.0	0.0	0.9	0.0
	Cj	0.0	0.0	0.0	100.0	0.0	0.0
	Mt	0.0	0.0	0.0	0.0	97.2	0.0
	Pp	0.0	0.0	0.0	0.0	0.0	100.0

the LBP-based system are completely different from the species misclassified by the GLCM-based method (Table 2). The CT images of *M. thunbergi* and *A. pictum* seem to be dissimilar, but these two species both have vessels are predominantly solitary with low density.

The results show that the LBP system performs better than the GLCM system. Because the textures appearing in the CT images are derived from the wood anatomical structure, which is composed of the cross section of the cell walls, the features of the cell shapes remain in the low-resolution images. Thus, the LBP method, which recognizes contours such as edges and corners, can capture the features of wood more effectively than the GLCM method, which considers only the relationship between two pixels. This also explains why the smoothing effect of the median filter works only on the LBP system; the median filter emphasizes the edges of the structure by removing the noise, but simultaneously loses some pixel gradient information because of the low resolution of the images. The LBP method has been used for wood identification using digital images or stereograms by several research groups [21–24], which evidences the suitability of the LBP method for discriminating wood structure.

## 5. Discussion

In this study, we investigated six diffuse-porous wood species used in the Tripitaka Koreana. In fact, the technique seems to be most suitable for the identification of wood used in culturally important objects in which the number of species used for a particular purpose is limited. This is partly because the property of

the material determines the quality of artifacts as well as because the craftsman selects materials based on his/her expertise, which is handed down from generation to generation. Therefore, this case study is a good example for curators, who may not be familiar with wood anatomy, because the CT technique is becoming a popular non-destructive and non-invasive way to investigate wooden artifacts. To facilitate the adoption of this useful technique, some examples of the R scripts and the image database used in this study are provided in the Supplementary Material.

The anatomists can do identification in the genus level empirically based on the systematic knowledge, however, the computer does it statistically based on the supervised database. The potential of the latter technique is tested by many researchers but still image database is not always enough to conclude how accurate this tool could be. Once again, the objective of the paper was to show availability of laboratory-scale CT machine for non-destructive wood identification. The use of median filtering to the reconstructed images and gray-level calibration to the density was found requisite. This means that one needs to record density calibration together with the objects. The accuracy of prediction is less important as it will certainly decrease when the computer studied more samples and learned similarities and variations between and within species. Therefore, the accuracy we reported is likely overestimated as we have only one wood sample for each species although the typical samples were selected carefully. Making database is another important task, and is in progress in cooperation with museum curators.

## 6. Conclusion

We presented a method for wood identification using a non-destructive method: the automatic image recognition of X-ray CT images. This method was demonstrated on wood used in the Tripitaka Koreana. The X-ray CT technique has been adopted in the cultural heritage field as a helpful non-destructive tool in the last decade. However, only part of the data that is visually recognizable has been utilized for investigations, even though the data in seemingly noisy regions should contain more information. Machine learning enables the analysis of such noisy data, which will increase the value of CT data, even data that already exists. Although deep learning is now a mainstream method for image recognition, traditional image recognition methods such as GLCM and LBP are suitable for many situations in the archaeological field where there is only a limited amount of data available and the number of candidate classifications is small.

## Acknowledgments

This study was supported by Grants-in-Aid for Scientific Research (Grant Number 25252033) from the Japan Society for the Promotion of Science, RISH Cooperative Research (database), and RISH Mission Research V. We thank Kim Moravec, PhD, from Edanz Group ([www.edanzediting.com/ac](http://www.edanzediting.com/ac)) for editing a draft of this manuscript.

## Références

- [1] IAWA Committee, IAWA List of Microscopic Features for Hardwood Identification, IAWA Bull. N. S. 10 (1989) 219–332.
- [2] IAWA Committee, IAWA list of microscopic features for softwood identification, IAWA J. 25 (2004) 1–70.
- [3] Y. Horikawa, S. Mizuno-Tazuru, J. Sugiyama, Near-infrared spectroscopy as a potential method for identification of anatomically similar Japanese diploxylons, J. Wood Sci. 61 (2015) 251–261, <http://dx.doi.org/10.1007/s10086-015-1462-2>.
- [4] S.W. Hwang, Y. Horikawa, W.H. Lee, J. Sugiyama, Identification of Pinus species related to historic architecture in Korea using NIR chemometric approaches, J. Wood Sci. 62 (2016) 156–167, <http://dx.doi.org/10.1007/s10086-016-1540-0>.

- [5] L.R. Schimleck, A.J. Michell, P. Vinden, Eucalypt wood classification by NIR spectroscopy and principal components analysis, *Appita J.* 49 (1996) 319–324.
- [6] S. Mizuno, R. Torizu, J. Sugiyama, Wood identification of a wooden mask using synchrotron X-ray microtomography, *J. Archaeol. Sci.* 37 (2010) 2842–2845, <http://dx.doi.org/10.1016/j.jas.2010.06.022>.
- [7] K. Kobayashi, M. Akada, T. Torigoe, S. Imazu, J. Sugiyama, Automated recognition of wood used in traditional Japanese sculptures by texture analysis of their low-resolution computed tomography data, *J. Wood Sci.* 61 (2015) 630–640, <http://dx.doi.org/10.1007/s10086-015-1507-6>.
- [8] S.-J. Park, A.-K. Kang, Species Identification of Tripitaka Koreana, *J. Korean Wood Sci. Technol.* 24 (1996) 80–89.
- [9] K. Kobayashi, S.W. Hwang, W.H. Lee, J. Sugiyama, Texture analysis of stereograms of diffuse-porous hardwood: identification of wood species used in Tripitaka Koreana, *J. Wood Sci.* 63 (2017) 322–330, <http://dx.doi.org/10.1007/s10086-017-1625-4>.
- [10] R.M. Haralick, K. Shanmugam, I. Dinstein, Textural features for image classification, *IEEE Trans. Syst. Man Cybern.* SMC 3 (1973) 610–621, <http://dx.doi.org/10.1109/TSMC.1973.4309314>.
- [11] N. Orlov, L. Shamir, T. Macura, J. Johnston, D.M. Eckley, I.G. Goldberg, WND-CHARM: Multi-purpose image classification using compound image transforms, *Pattern Recogn. Lett.* 29 (2008) 1684–1693, <http://dx.doi.org/10.1016/j.patrec.2008.04.013>.
- [12] L. Shamir, N. Orlov, D.M. Eckley, T. Macura, J. Johnston, I.G. Goldberg, Wndchrm – an open source utility for biological image analysis, *Source Code Biol. Med.* 3 (2008) 13, <http://dx.doi.org/10.1186/1751-0473-3-13>.
- [13] T. Okochi, A nondestructive dendrochronological study on Japanese wooden shinto art sculptures using micro-focus X-ray Computed Tomography (CT): reviewing two methods for scanning objects of different sizes, *Dendrochronologia* 38 (2016) 1–10, <http://dx.doi.org/10.1016/j.dendro.2016.01.004>.
- [14] T. Ojala, M. Pietikäinen, D. Harwood, A comparative study of texture measures with classification based on featured distributions, *Pattern Recognit.* 29 (1996) 51–59, [http://dx.doi.org/10.1016/0031-3203\(95\)00067-4](http://dx.doi.org/10.1016/0031-3203(95)00067-4).
- [15] T. Ojala, M.P.T. Mäenpää, Multiresolution gray-scale and rotation invariant texture classification with local binary patterns, *IEEE Trans. Pattern Analysis Machine Intelligence* 24 (2002) 971–987, <http://dx.doi.org/10.1007/3-540-45054-8-27>.
- [16] R Core Team, R: A language and environment for statistical computing, (2016). R Foundation for Statistical Computing, Vienna, Austria. <https://www.R-project.org/>.
- [17] S. Urbanek, tiff: Read and write TIFF images, (2013). <https://CRAN.R-project.org/package=tiff>.
- [18] B. Ripley, W. Venables. class: functions for classification, (2019). <https://CRAN.R-project.org/package=class>.
- [19] J. Sugiyama, K. Kobayashi, wvtool: Image tools for automated wood identification, (2016). <https://CRAN.R-project.org/package=wvtool>.
- [20] F. Albrechtsen, Statistical texture measures computed from gray level cooccurrence matrices, technical note, Department of Informatics. (2014) 1–14.
- [21] P.R. Cavalin, M.N. Kapp, J. Martins, L.E.S. Oliveira, A multiple feature vector framework for forest species recognition, in: Proceedings of the 28th Annual ACM Symposium on Applied Computing, ACM, New York, USA, 2013, pp. 16–20, <http://dx.doi.org/10.1145/2480362.2480368>.
- [22] J.G. Martins, L.S. Oliveira, A.S. Britto, R. Sabourin, Forest species recognition based on dynamic classifier selection and dissimilarity feature vector representation, *Mach. Vis. Appl.* 26 (2015) 279–293, <http://dx.doi.org/10.1007/s00138-015-0659-0>.
- [23] A.R. Yadav, R.S. Anand, M.L. Dewal, S. Gupta, Analysis and classification of hardwood species based on Coiflet DWT feature extraction and WEKA workbench, in: 2014 International Conference on Signal Processing and Integrated Networks (SPIN), IEEE (2014) 9–13, <http://dx.doi.org/10.1109/SPIN.2014.6776912>.
- [24] A.R. Yadav, R.S. Anand, M.L. Dewal, S. Gupta, Multiresolution local binary pattern variants based texture feature extraction techniques for efficient classification of microscopic images of hardwood species, *Appl. Soft Comput.* 32 (2015) 101–112, <http://dx.doi.org/10.1016/j.asoc.2015.03.039>.